

AIAA 81-0011R

# Analysis of Lift Losses for a Round Planform with a Central Jet

K.T. Yen\*

*Aircraft and Crew Systems Technology Directorate, Naval Air Development Center, Warminster, Pa.*

An analysis of the lift losses for a round planform fitted with a centrally located round jet is presented. The pressure distribution over the lower surface of the planform is solved analytically by matching an inner viscous solution with an outer potential solution. By comparing the calculated pressure distributions with NACA experimental data, satisfactory agreement has been obtained, although the planforms are not exactly the same. In addition, Wyatt's formula for the lift losses is found to be essentially valid, but only under limited conditions; as a result, an improved formula is suggested. Additional works, both experimental and theoretical, needed to solve the lift loss problem are recommended.

## Nomenclature

$d$	= exit diameter of jet
$D$	= diameter of planform
$\bar{D}$	= equivalent diameter of planform
$h$	= height of planform from ground plane
$HR$	= height Reynolds number $= \rho Vh/\mu$
$JR$	= jet Reynolds number $= \rho Vd/\mu$
$-p$	= static pressure
$-p_i$	= static pressure at jet exit
$p_{i0}$	= dimensionless static pressure at jet exit $= -p_i/P$
$P$	= pressure parameter $= T/8\pi h^2$
$q$	= strength of source flow
$r$	= radial distance from jet centerline
$r_0$	= radius of jet exit $= d/2$
$R_0$	= dimensionless jet exit radius $= d/D$
$Re$	= Reynolds number defined as $\rho VD/\mu$
$S$	= lift loss
$T$	= thrust of jet
$v$	= radial velocity
$V$	= mean exit velocity of jet
$\lambda$	= entrainment factor
$\mu$	= coefficient of viscosity
$\nu$	= kinematic viscosity
$\rho$	= density
$\phi$	= velocity potential

## Introduction

THE problem of lift losses for V/STOL aircraft in hovering flight, critically important to their development and design, has been reviewed by Margason<sup>1</sup> and by Walters and Henderson.<sup>2</sup> Although a variety of prediction methods for the jet-induced lift losses is available, ranging from essentially complete reliance on testing to complex computerized methods, both the accuracy and reliability of these methods have been found deficient when their results are compared with experimental data (see, e.g., Ref. 2). Although this is because of an insufficient data base in some cases, the inadequacies of the methods in terms of aerodynamic modeling and analytical basis also play a significant part.

Multiple lifting jets in ground effect may produce a fountain which, upon impingement on the aircraft, can supply a lift increment. The net lift loss for this case is the difference between the jet-induced suckdown force and the

fountain lift increment. An analysis of the fountain lift increment has been presented in Ref. 3. In the present work, an analytical solution of the suckdown for a round planform with a centrally located single lifting jet is reported. A study of the multijet suckdown will be reported elsewhere.<sup>4</sup>

In the prediction methods developed by Kuhn<sup>5</sup> and by Karema and Ramsey,<sup>6</sup> the basic analytical tool is a formula of the lift losses for an "equivalent single jet" (i.e., a single jet with an equivalent circular planform). However, these formulas have been obtained entirely from correlating experimental data. Not only have different empirical approaches yielded different formulas for the lift losses, but "discrepancy between the results from two apparently almost identical experiments" has also been found by Wyatt.<sup>7</sup>

The present work is basically analytical. The pressure distribution over the planform is determined by matching a potential solution with a viscous solution. By numerical integration of the pressure distribution, the suckdown force is obtained. An analysis of the present results has substantiated to a large extent Wyatt's formula for the lift losses, but its limitations, as well as needed improvements, can be identified. In the present analysis, the emphasis is on the basic aerodynamic features of the problem, and only circular planforms will be considered.

## Experimental Work

An experimental study of the lift losses for single-jet configurations (i.e., single jets issuing from various circular, rectangular, and triangular plates) has been conducted by Wyatt.<sup>7</sup> His formula for the lift loss (referred to out-of-ground effect) is

$$S/T = 0.012 [h/(\bar{D} - d)]^{-2.3} \quad (1)$$

For a centrally located jet in a circular planform,  $\bar{D} = D$ . The geometrical parameters in Wyatt's experiments are as follows (approximately):  $0.1 \leq d/D \leq 0.3$ ;  $0.15 \leq h/D \leq 1.2$ . In addition, the values of the jet Reynolds number  $JR = Vd/\nu$ , where  $V$  is a mean jet efflux velocity and  $\nu$  the kinematic viscosity coefficient, are in the range  $(1.0-3.1) \times 10^6$ .

Wyatt was unable to correlate his results with those from an earlier work by Spreemann and Sherman.<sup>8</sup> He found that application of Eq. (1) to NACA results in Ref. 8 required that the power index be changed to  $-2.02$  and the proportional constant to  $0.025$ . In addition to the lift losses, the induced pressures on the lower surface of two square plates were measured by Spreemann and Sherman. Their graphs show the pressure distributions dependent on the values of  $h/d$  and the plate size. An examination of the pressure distributions suggests that there are two distinct regions of different aerodynamic characteristics.

Presented as Paper 81-0011 at the AIAA 19th Aerospace Sciences Meeting, St. Louis, Mo., Jan. 12-15, 1981; submitted March 6, 1981; revision received Sept. 30, 1981. Copyright © American Institute of Aeronautics and Astronautics, Inc., 1981. All rights reserved.

\*Adjunct Professor. Present address: Radnor Center for Graduate Studies and Continuing Education, The Pennsylvania State University, Radnor, Pa.

The induced-pressure distributions on the lower surface of a 101.6-cm (40-in.) diameter disk with a 2.54-cm (1-in.) jet diameter at three values of  $h$ , that is, at 12.7, 7.62, and 5.08 cm (5, 3, and 2 in.) have also been measured by Gelb and Martin found that at a height of 5.08 cm (2 in.), the jet filled the annular space and the flow became "a radial uniform flow." At a height of 12.7 cm (5 in.), there was an inflow toward the jet exit over a substantial portion of the lower surface of the disk.

### Analysis: Matched Potential and Viscous Solution for the Pressure Distribution

In Fig. 1, two streamline patterns for the jet-induced flowfield near a circular plate are shown. Figure 1a shows a purely radial flow expected to be valid for  $h/D \ll 1$ , as found by Gelb and Martin for  $h/D = 0.05$ . The flow pattern in Fig. 1b, consistent with that obtained by Gelb and Martin with  $h/D = 0.125$  and  $d/D = 0.05$ , is designated as the case  $h/D < 1$ . Its range of validity may extend to  $h/D \sim 0.5$ , depending on the jet Reynolds number.

The pressure distributions over the lower surface of the plate are also sketched in Fig. 1. These distributions are in general accord with the experimental evidences. In particular, both distributions are shown to have two distinct regions with unique, but different, aerodynamic characteristics. The inner and outer regions of pressure distribution can be considered as viscous and potential pressure distributions, respectively, since their main features can be defined by the viscous and potential flow solutions to be presented in the following.

It must be added that Figs. 1a and 1b are not the only possible flow patterns under the condition  $h < D$ . As pointed out by Spreemann and Sherman,<sup>8</sup> a trapped doughnut-shaped vortex may form under the plate, depending primarily on the size of the plate (i.e., on the value of  $d/D$ ). For such a trapped vortex flow pattern, the pressure distribution appears to be largely of a viscous nature, and no potential pressure

region is present [see Fig. 19b in Ref. 8 for a 15.24-cm (6-in.) square plate, with  $d/\bar{D} = 0.1667$  and  $h/d = 1.0$ ]. It is expected, however, that, subject to further study, the trapped doughnut-shaped vortex occurs at values of  $h/\bar{D}$  lying between those for Figs. 1a and 1b, and only for limited values of  $d/\bar{D}$ . Consequently, the trapped vortex flow pattern will not be treated in the present study. Of course, the results presented here may be inadequate at such values of  $d/\bar{D}$ .

### Potential Pressure Distribution

An examination of the flow shown in Fig. 1a suggests the use of a potential source to describe the flow in the annular space in the outer region. For Fig. 1b, it is proposed to approximate the flow close to the lower surface in the outer region by a potential sink flow. The potential pressure distribution is to be matched with a viscous distribution in the inner region, and the extent of the region of validity for the potential flow will be determined.

The velocity potential of a source or sink is

$$\phi = (q/2\pi)(\log r + C) \quad (2)$$

where  $q$  is the strength of the source (positive) or sink (negative),  $r$  is the radial distance, and  $C$  is an arbitrary constant. The radial velocity is

$$v = \frac{d\phi}{dr} = \frac{q}{2\pi} \frac{1}{r} \quad (3)$$

The static pressure  $-p$  is given by

$$p = p_0 - \rho \left( \frac{q}{2\pi} \right)^2 \frac{1}{2r^2} \quad (4)$$

where  $p_0$  is a constant. By taking  $p = 0$  at  $D/2$ ,  $p_0$  is found to be

$$p_0 = 2\rho \left( \frac{q}{2\pi} \right)^2 \frac{1}{D^2}$$

Thus in the outer region the pressure is

$$p = -\frac{\rho}{2} \left( \frac{q}{2\pi} \right)^2 \left( \frac{1}{r^2} - \frac{4}{D^2} \right) \quad (5)$$

For  $h/D \ll 1$  (Fig. 1a), the strength  $q$  can be determined from the conservation relation  $\pi r_0^2 V = qh$ , where  $r_0 = d/2$ . For the case  $h/D < 1$ , shown in Fig. 1b, the inflow is produced by the jet entrainment of the ambient fluid. In the absence of adequate information for the entrainment, a dimensional analysis has yielded the following modified conservation relation:

$$\pi r_0^2 V = \lambda qh \quad (6)$$

where  $\lambda$  is a dimensionless entrainment factor found to be generally greater than 1; however, it approaches 1 as  $h$  becomes small. The entrainment factor should, in general, depend on  $JR$  and  $d/D$  as well as  $h/D$ .

It is convenient to refer the lift loss to the jet thrust  $T = \pi r_0^2 \rho V^2$ , and to nondimensionalize the pressures with respect to

$$P = T/8\pi h^2 \quad (7)$$

Consequently, in the outer region, the pressure is given by

$$\frac{p}{P} = -\frac{r_0^2}{\lambda^2} \left( \frac{1}{r^2} - \frac{4}{D^2} \right) \quad (8)$$

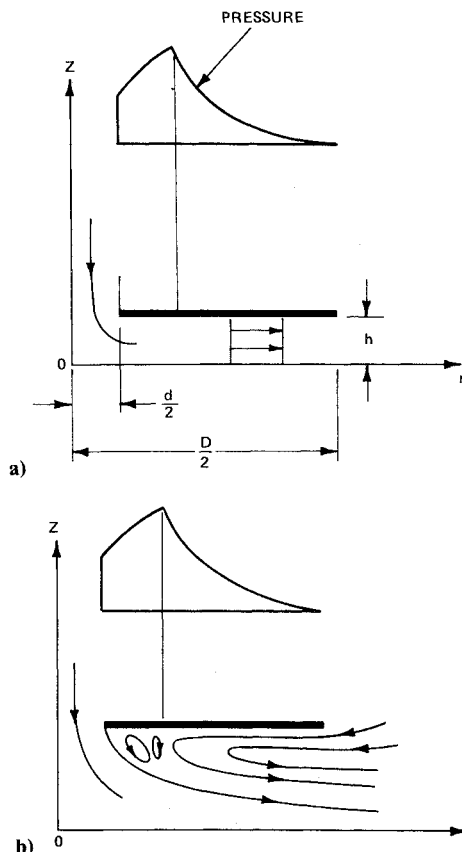


Fig. 1 Flow patterns induced by the jet. a)  $h/D \leq 1$ ; b)  $h/D < 1$ .

### Viscous Pressure Distribution

It is well known that when the plate is close to the ground plane ( $h/D \ll 1$ ), the solution of the flow can be simplified (see, e.g., Ref. 10). The pressure is related to the velocity potential by the following formula:

$$p = -(12\mu/h^2)\phi \quad (9)$$

where  $\mu$  is the coefficient of viscosity. Thus, using Eq. (2),

$$p = \frac{12\mu}{h^2} \frac{q}{2\pi} \log\left(\frac{r}{r_0}\right) + p_i \quad (10)$$

where  $p_i$  is the static surface pressure at the jet exit. Spreemann and Sherman's measurements show  $p_i$  dependent on  $h/d$ ; it may also vary with the jet Reynolds number and with the ratio  $d/D$ . However,  $p_i$  is not well defined at this time, and it is considered as a parameter in the present analysis. In dimensionless form, the viscous pressure in the inner region for the case  $h/D \ll 1$  is

$$\frac{p}{P} = -\frac{48}{HR} \frac{1}{\lambda} \log\left(\frac{r}{r_0}\right) - p_{i0} \quad (11)$$

where  $HR$  is the height Reynolds  $\rho Vh/\mu$  and  $p_{i0} = -p_i/P$ .

The pressure distributions (8) and (11) for the outer and inner regions evidently are only approximations obtained by an heuristic analysis. Now the nature of the approximations will be examined. Moller<sup>11</sup> has obtained a solution for the turbulent pressure distribution (between two parallel disks), using an integral momentum method for the case  $h/d \ll 1$  ( $\lambda = 1$ ). Moller's solution can be written in the following form:

$$\begin{aligned} \frac{p}{P} = & -1.016r_0^2 \left( \frac{1}{r^2} - \frac{4}{D^2} \right) + 0.297284 \frac{r_0^2}{hD} \\ & \times \left( \frac{1}{Re} \right)^{1/4} \left[ \left( \frac{D}{r} \right)^{3/4} - 1.682 \right] \end{aligned} \quad (12)$$

The first term on the right-hand side of Eq. (12) is essentially the potential pressure (8). Consequently, the pressure distribution (8) may be regarded as an asymptotic solution for high values of the Reynolds number.

Moller has compared his experimental results with the pressure distribution over the disk. He found good agreement in the outer region, but not in the inner region. It is significant that the "potential pressure," even with a viscous correction term as given in Eq. (12), is still not applicable to the inner region, based on Moller's analysis. In the present analysis, the potential pressure is not applied to the inner region. Instead, a method of viscous and potential pressure matching is used in the absence of an analytical solution valid in both the inner and outer regions.

With the existence of a viscous pressure region accepted, an accurate determination of the solution by accounting for all viscous and inertia effects, including turbulence and flow separation (but not compressibility), is, however, not an easy task. The distribution given in Eq. (11) is the well-known slow-motion solution without inertia effects. Although the solution is not entirely satisfactory, as will be seen, it appears to be adequate for the present study of lift losses.

For the case of  $h/D < 1$ , that is,  $\lambda > 1$ , there appears to have been very little theoretical work done on the pressure distribution. The viscous solution given by Eq. (11) is, strictly speaking, not applicable. However, in the inner region, the flow has under certain conditions (e.g., at large values of  $Re$ ) the characteristics of a dead-water region, and the pressure variation is small. Thus the use of such a simple solution is considered acceptable at this time.

The outer pressure solution (8) is always negative, but the viscous term in Eq. (12) is positive. At small values of  $Re$  or

$h/D$ , the viscous term becomes more important and the outer solution (12) may become positive. The inner pressure solution (11) is negative at negative values of  $p_i$  (or positive values of  $p_{i0}$ ). If  $p_i$  is positive and sufficiently large, a substantial portion of the inner pressure will be positive. Moller's measurements show that the pressure is positive when the flow is laminar and negative when the flow is turbulent ( $h/d \ll 1$ ). It is possible, therefore, that in general  $p_i$  is positive when the flow is laminar and negative when the flow is turbulent. For the lift-loss problem, the flow is considered turbulent with negative values of  $p_i$  (i.e., positive  $p_{i0}$ ). Evidently, when the flow is laminar, there will be a lift increment, as is generally known to be the case when  $h/D$  is very small compared with 1.

### Numerical Results and Comparison with Experimental Data

From the above analysis, the following significant parameters for the lift loss of a circular flat planform with a centrally located jet can be identified:

- 1)  $d/D$
- 2)  $h/D$
- 3)  $p_{i0}$
- 4)  $JR$
- 5)  $\lambda$

The height Reynolds number,  $HR = \rho Vh/\mu$ , evidently can be written as the product of  $JR$ ,  $h/D$ , and  $D/d$ . However, in the numerical evaluation of the present solution, it is more convenient to use  $HR$ . In fact, the lift loss can be written in the following functional form:

$$\frac{S}{T} = \frac{D^2}{h^2} f\left(\frac{d}{D}, HR; \lambda, p_{i0}\right) \quad (13)$$

The above formula shows that the dependence of the lift loss on the height  $h$  derives from two parts,  $h^{-2}$  and  $HR$ . Thus the power  $-2.3$  in Wyatt's work may be only of limited validity. The following numerical analysis will prove that this is indeed the case. In addition, the power of  $(D-d)^{-1}$  is found to be generally different from that of  $h$ . It is noted that the two quantities  $\lambda$  and  $p_{i0}$  normally are not dimensionless parameters of the lift-loss problem. If it is possible to determine these two quantities from an analysis, the only dimensionless parameters will be  $D/h$ ,  $d/D$ , and  $HR$ .

Numerical evaluation of the solution has been carried out for a large number of cases with  $d/D$  and  $p_{i0}$  in the following ranges:

$$0.00 < d/D < 1.00$$

$$0.00 < p_{i0} < 0.20$$

The values of  $HR$  are divided into two categories: "low-height" Reynolds number,  $HR$ 's from 100 to 1000; and "high-height" Reynolds number,  $HR$ 's from  $10^4$  to  $10^6$ . The numerical results will be presented in these two categories. However, few experimental data for the low- $HR$  category are available, and only the high- $HR$  case is of primary interest in V/STOL aircraft technology. Consequently, only the high- $HR$  results will be compared with the experimental data obtained by Wyatt, and by Spreemann and Sherman.

#### Low-Height Reynolds Number

For low-height Reynolds numbers, with values ranging from 100 to 1000 (to 4000 in some cases), the entrainment factor  $\lambda$  equals 1. In fact, jet entrainment plays no role in the suckdown or lift loss for this case.

Typical pressure distributions are shown in Figs. 2 and 3. Note the changes in the viscous portion of the distributions as the height Reynolds number is increased. The potential pressure portion, however, remains the same.

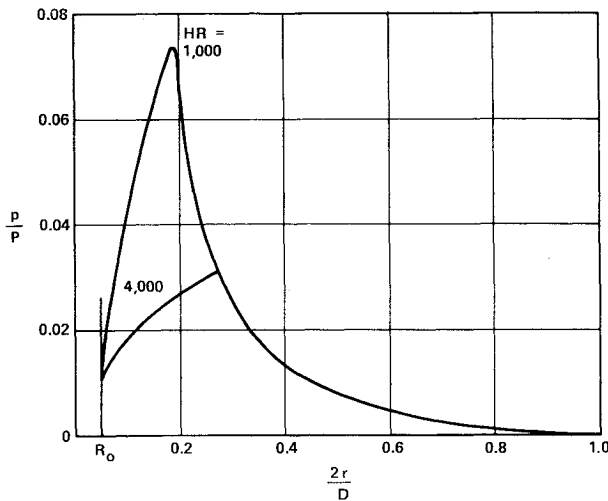


Fig. 2 Surface pressure distributions for  $HR=1000$  and  $4000$ ;  $p_{i0}=0.01$ .

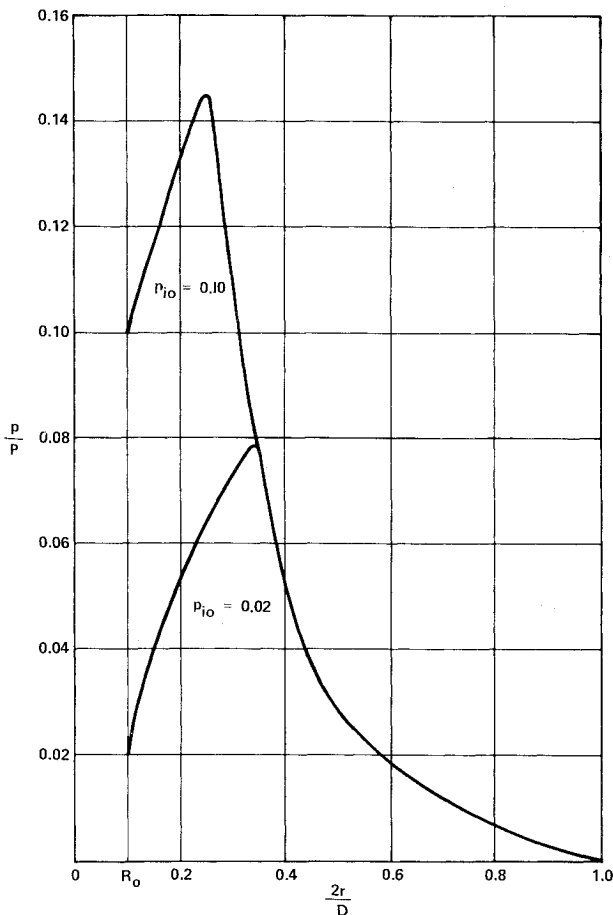


Fig. 3 Surface pressure distributions for  $HR=1000$ ;  $p_{i0}=0.02$  and  $0.1$ .

The lift loss in terms of  $h^2 S / 16 \pi D^2 T$  plotted vs  $(1 - d/D)^2$  for various values of  $HR$  and  $p_{i0}$  is given in Figs. 4-6. Some significant features of these results should be noted. First of all, the lift loss is shown to vanish at both ends of the  $(1 - d/D)^2$  scale; that is, for  $d/D=0$  and  $1.0$ . Thus the suckdown force generally has a peak, which for  $HR=500$  and  $p_{i0}=0.02$  occurs close to  $(1 - d/D)^2=0.5$  or  $d/D=0.293$  (Fig. 5). These peaks shift to higher or lower values of  $(1 - d/D)^2$  as  $p_{i0}$  decreases or increases. On the other hand, the peak moves to a higher value of  $(1 - d/D)^2$  as  $HR$  increases. In addition, the larger the value of  $p_{i0}$  the larger is the lift loss.

Figures 4-6 show that the lift loss depends on the height Reynolds number. Thus, in addition to the power  $h^{-2}$ , the lift loss also varies with  $h$  through  $HR = \rho V h / \nu$ , as can be seen from Fig. 7. It is of interest to note, however, that this dependence is not in the form of a single power. At a value of  $d/D=0.05$ , the dependence can be approximated by  $-0.2$  power. At  $d/D=0.2$ , the power is found to be  $-0.33$ . This is illustrated graphically in Fig. 8, in which the factor  $HR^{0.3}$  is introduced to the lift loss to determine if a power  $-2.3$  for  $h$  is an adequate approximation. Since the three curves for  $HR=500$ ,  $1000$ , and  $3000$  do not reduce to a single curve, clearly this approximation is not uniformly valid over the whole range  $0 < d/D < 1.0$ . In the region near the peak suckdown, the deviation can be as large as 10% from the mean.

In Moller's experiments for a sharp-edged entry and  $D/d$  equal to 6 at  $JR=12,200$  (Fig. 3 of Ref. 11), the height Reynolds number,  $HR$ , has the range of approximately 508.7-812.5. The experiments belong to the low- $HR$  category. However, in the figure for the turbulent pressure distribution, no data are given in the inner region near the entry. Thus a comparison of Moller's experimental data with the present pressure solution is not possible. It is noted that when plotted in the form of  $p/P$  vs  $2r/D$ , the four pressure distributions for four values of  $h/D$  given by Moller nearly collapse into one curve. Thus the viscous correction for the potential pressure is not significant in these cases.

#### High-Height Reynolds Number

In Wyatt's experiments, the height Reynolds number covers the range from  $HR=5.0 \times 10^5$ - $3.72 \times 10^7$ . According to Wyatt, in Spremann and Sherman's work the jet Reynolds number is  $0.5 \times 10^6$  compared with  $(1.0-3.1) \times 10^6$  in his work. Consequently, the measurements by Wyatt and by Spremann and Sherman are in the high-height Reynolds number range.

To make computations using Eqs. (6), (8), and (11) for this case it is necessary to know the value of the entrainment factor  $\lambda$  as a function of  $JR$ ,  $d/D$ , and  $h/D$ . Such information is not available, and in the present work several constant values of  $\lambda$  are used in the analysis.

From Eqs. (8) and (11), it is observed that as  $\lambda$  is increased from  $\lambda=1$  to larger values, the magnitude of both the potential and viscous pressures will reduce in magnitude. The reduction in the potential pressure will be larger, since it is proportional to  $\lambda^{-2}$  instead of  $\lambda^{-1}$  in the viscous pressure. The magnitude of the lift loss will consequently drop in a nonlinear manner when  $\lambda$  increases.

For illustration, Figs. 9 and 10 show the comparison between the pressure distributions measured by Spremann and Sherman (Fig. 19a, Ref. 8) and those calculated by using values of  $p_{i0}$  given in Ref. 8 for several values of  $\lambda$ . The measurements were made for a 25.4-cm (10-in.) square plate with  $d/\bar{D} \approx 0.10$ ; the results for  $h/d=1.0$  are shown in Fig. 9, and those for  $h/d=0.5$  are shown in Fig. 10. The calculated results in Fig. 9 are for  $HR=10^4$  and for  $\lambda=1.0$  and  $1.2$ ; in Fig. 10 they are for  $\lambda=2.0$ ,  $2.2$ , and  $2.5$ . The agreement between the measurements and calculations appears to be good, at least qualitatively.

However, some significant points should be noted. In the present analysis, the pressure is assumed to have the ambient value at the edge of the plate. This is consistent with the results of Gelb and Martin. But Ref. 8 gives no pressure data at the plate edge. In addition, the pressure distributions for  $h/d=2.0$  and  $4.0$  in Fig. 19a of Ref. 8 do not contain enough detail to show any definitive pattern—viscous, viscous-potential, or otherwise. Whether they reach the ambient value at the plate edge is uncertain. Although these two cases of higher  $h/d$  values are of interest to the lift-loss problem, no meaningful evaluation or comparison appears possible without additional, more accurate measurements. Moreover, there is no reason to expect that these two distributions will be other than the viscous-potential type shown in Fig. 1b.

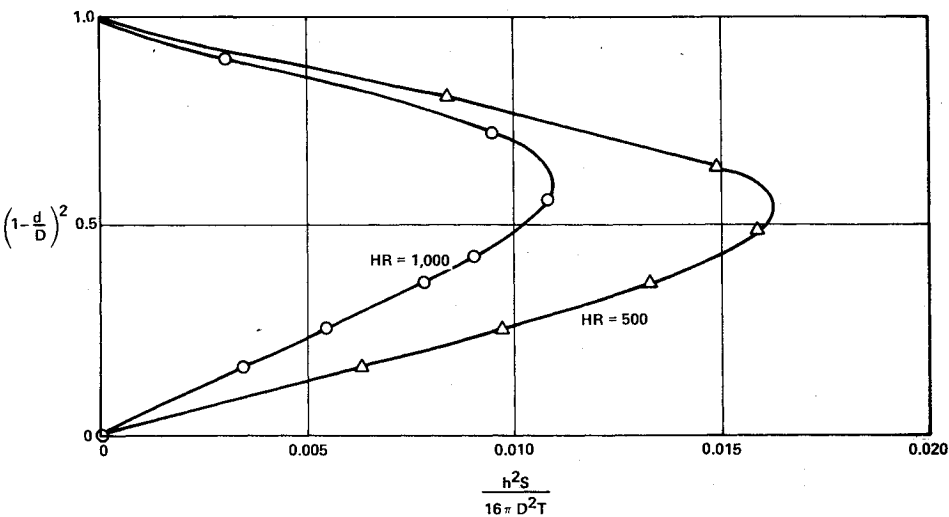


Fig. 4 Lift loss  $h^2 S/16 \pi D^2 T$  for  $p_{i0} = 0$ .

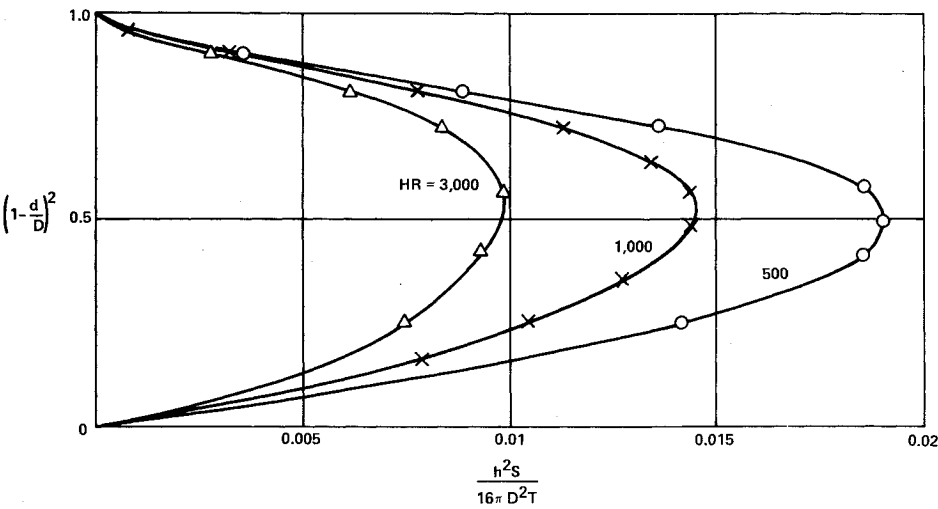


Fig. 5 Lift loss  $h^2 S/16 \pi D^2 T$  for  $p_{i0} = 0.02$ .

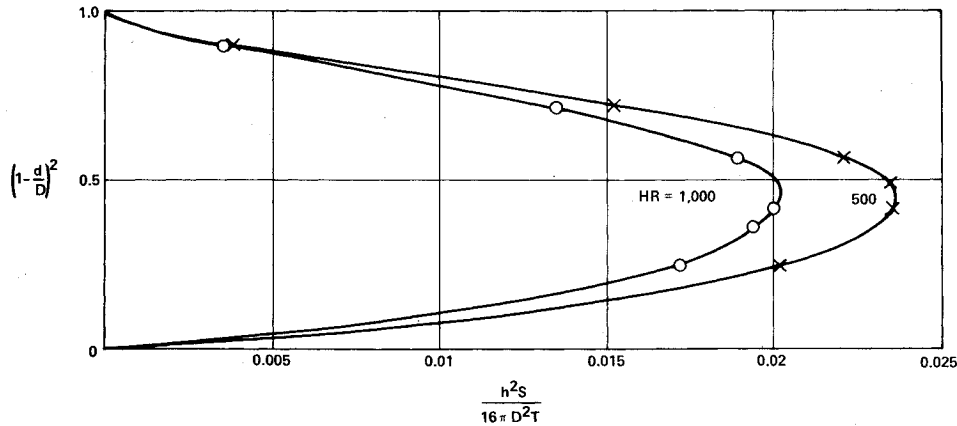


Fig. 6 Lift loss  $h^2 S/16 \pi D^2 T$  for  $p_{i0} = 0.05$ .

It is of interest to point out that a method of determining the entrainment factor  $\lambda$  is to measure the surface pressures and compare them with calculations for several well-chosen values of  $\lambda$ . The correct  $\lambda$  value is that yielding the best agreement between the measurements and calculations. Although the agreement shown in Figs. 9 and 10 appears to be satisfactory, the results do not necessarily constitute an accurate determination of  $\lambda$  for the present cases.

Irrespective of the uncertainty in the entrainment factor  $\lambda$ , the general characteristics of the lift loss can be stated as follows:

- 1) The lift loss  $h^2 S/16 \pi D^2 T$  plotted vs  $(1 - d/D)^2$ , with

$HR$  and  $p_{i0}$  as parameters, vanishes at both ends of the scale, that is, for  $d/D = 0$  and  $1.0$ .

- 2) The lift loss has a peak at some immediate value of  $d/\bar{L}$ , depending on  $HR$  and  $p_{i0}$ . For example,  $h^2 S/16 \pi D^2 T$  peaks at  $d/D = 0.245$  for  $HR = 10^6$  and  $p_{i0} = 0.01$  (with  $\lambda = 1.0$ ).
- 3) In addition to  $h^{-2}$ , the lift loss  $S$  varies with  $h$  through the height Reynolds number. This additional dependence is compared with Wyatt's  $-0.3$  power in Fig. 11. These characteristics are of the same nature as those for the low- $HR$  case.

A typical plot of the lift loss vs  $(1 - d/D)^2$  is given in Fig. 12. To use such graphs for analysis, it is necessary to know the

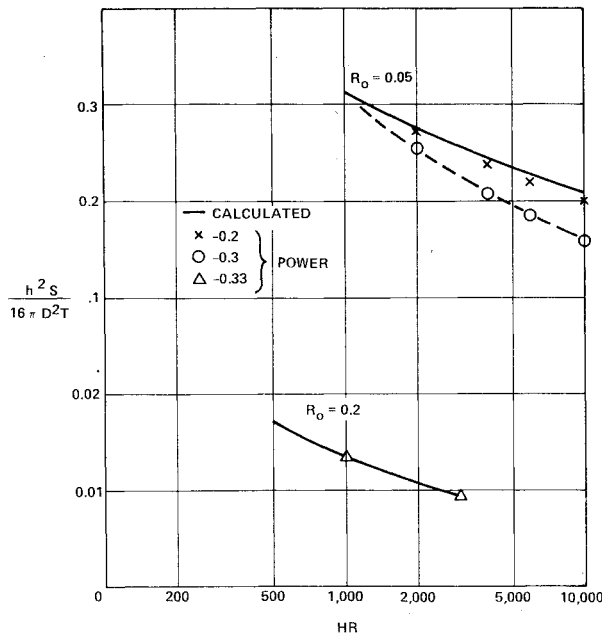


Fig. 7 Dependence of  $h^2 S / 16\pi D^2 T$  on  $HR$  - low  $HR$ .

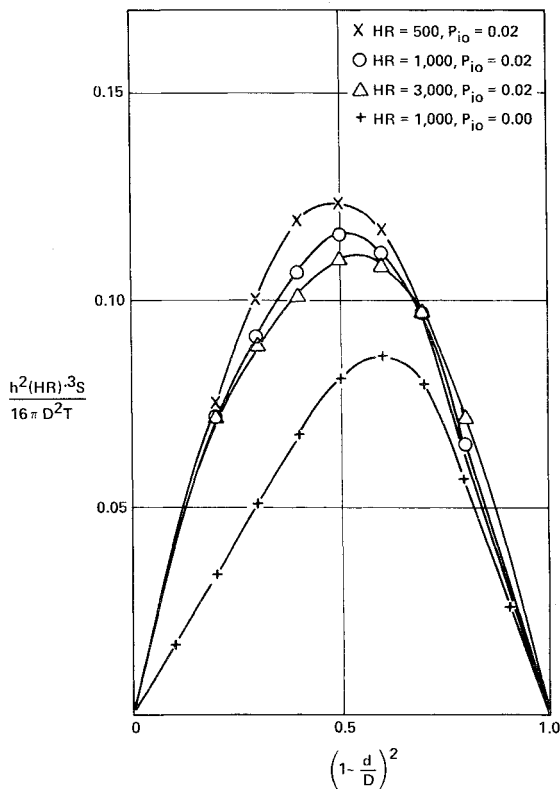


Fig. 8 Lift loss  $h^2 (HR)^{0.3} / 16\pi D^2 T$  vs  $(1 - d/D)^2$ .

parameters  $p_{i0}$  and  $\lambda$  for given values of  $HR$  and  $d/D$ . This requires additional study beyond the scope of the present analysis.

To make a comparison with Wyatt's experimental results, it is convenient to present the results in the form of  $Sh^{2.3}/T$  as a function of  $(1 - d/D)^{2.3}$ . It is noted, however, in reducing the numerical data that the jet Reynolds number, the height Reynolds number,  $h/D$ , and  $d/D$  are related. To be consistent, the following procedure is used. First, the thrust of the jet is kept constant as  $d/D$  is changed. Thus  $Vd/D$  is maintained as a constant. Second, define a Reynolds number,  $Re = \rho V D / \mu$ , and take  $Re = 10^7$  at  $d/D = 0.02$ . Then at any

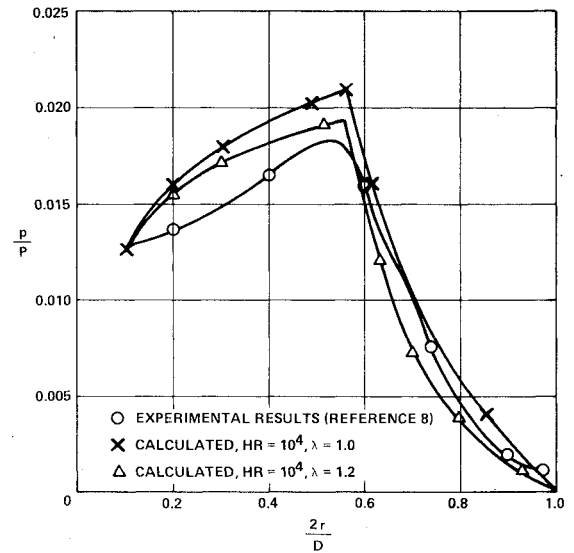


Fig. 9 Surface pressure distributions,  $p_{i0} = 0.01267$ .

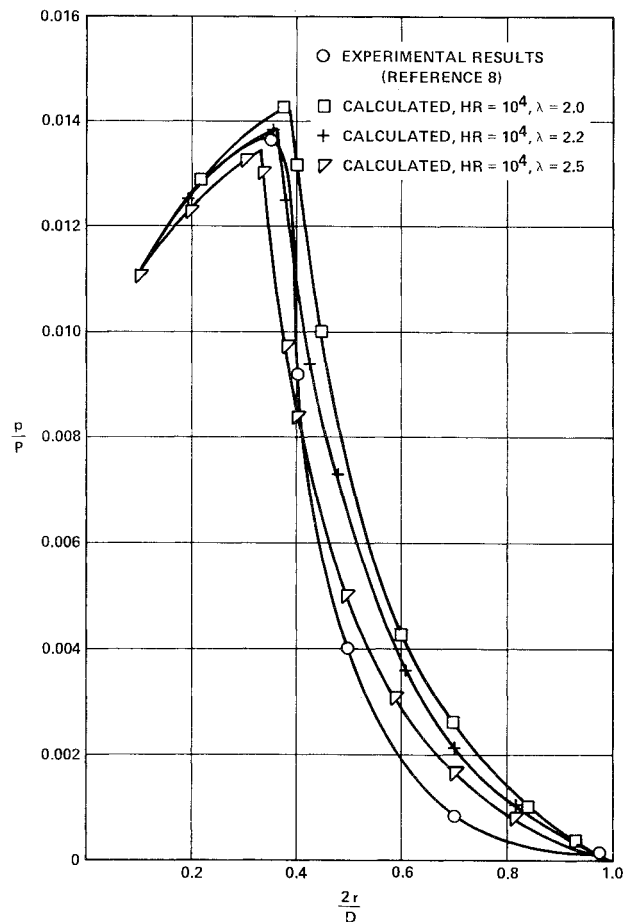


Fig. 10 Surface pressure distributions,  $p_{i0} = 0.01108$ .

other  $d/D$ , the value of  $Re = (D/5d)^2 \times 10^7$ . An example of such a data reduction is shown in Fig. 13 for  $HR = 10^5$ ,  $p_{i0} = 0.001$ , and  $\lambda = 1.0$ . In Fig. 13, Wyatt's formula, Eq. (1), becomes a straight line, although his experimental data cover only a limited range. These two graphs intersect at the point I. Thus, based on the present results, the surface pressure at the jet exit  $p_{i0}$  for  $(1 - d/D)^{2.3} = 0.615$  or  $d/D = 0.1905$  has the value of 0.001. No data for  $p_{i0}$  were given in Wyatt's report.

In view of the uncertainties involving the parameters, the use of Wyatt's formula for the determination of  $p_{i0}$  does not

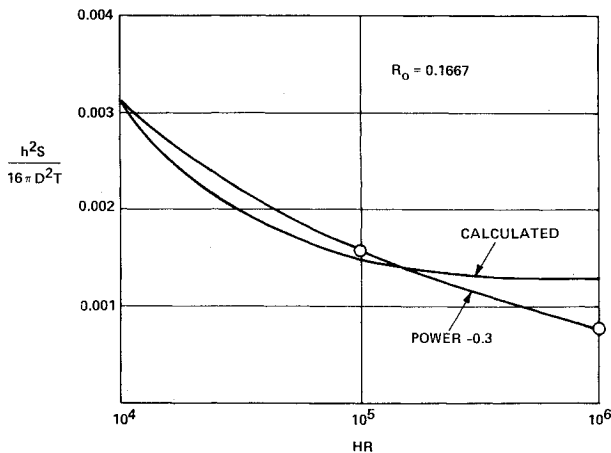


Fig. 11 Dependence of  $h^2 S / 16 \pi D^2 T$  on  $HR$  - high  $HR$ .

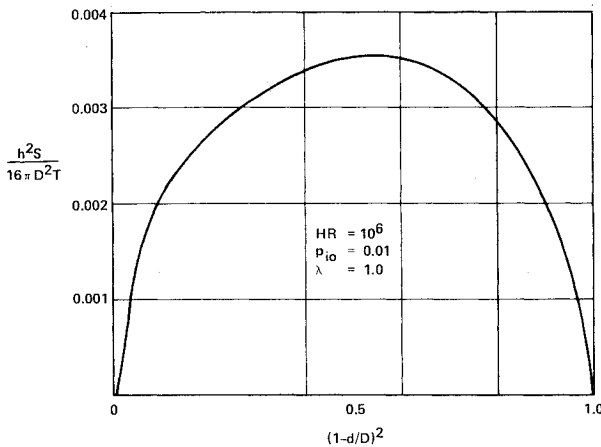


Fig. 12 Lift loss  $h^2 S / 16 \pi D^2 T$ ,  $HR = 10^6$ ,  $p_{i0} = 0.01$ , and  $\lambda = 1.0$ .

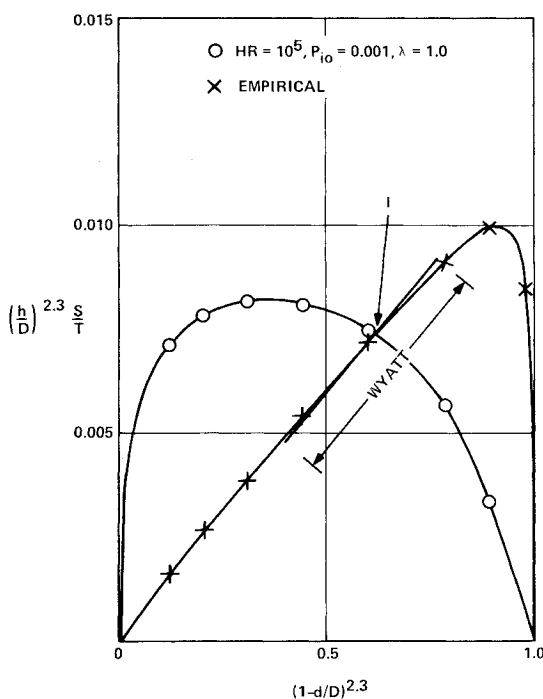


Fig. 13 Lift loss  $(h/D)^{2.3} S/T$  vs  $(1-d/D)^{2.3}$ .

appear meaningful. Instead, the following empirical formula is proposed:

$$\left(\frac{h}{D}\right)^{2.3} \frac{S}{T} = 0.013 \left(\frac{d}{D}\right)^{0.05} \left(1 - \frac{d}{D}\right)^{2.25} \quad (14)$$

Figure 13 shows the above formula to be a good approximation to Wyatt's. This formula has the characteristic that it vanishes at  $d/D = 0$  and  $1.0$ . Additional improvements, however, are needed to include, for example, the effects of the jet Reynolds number.

From the above comparison, the following can be stated:

1) Wyatt's formula may have only a limited range of validity in the values of  $d/D$  and  $JR$ , and it does not predict peak suckdown forces, which appear (based on the present analysis) to exist.

2) The power  $-2.3$  for  $h$  in Wyatt's formula can be considered as an acceptable approximation in limited ranges of the parameters.

3) There is no evidence that the factor  $(1-d/D)$  should have the power of  $2.3$ . The dimensionless quantities  $h/D$  and  $1-d/D$  are independent of each other.

### Conclusions and Recommendations

A method of viscous and potential pressure matching has been used for an analysis of the lift-loss problem for a round planform with a central lifting jet and Wyatt's formula for the lift losses. The analysis shows that viscous effects contribute significantly to the lift losses. In fact, it was found that in Wyatt's formula for  $S/T$ , of the  $h^{-2.3}$  dependence at least  $h^{-0.3}$  is due to viscous effects, while the potential flow effects cannot exceed  $h^{-2.0}$ .

Two quantities in the problem cannot be predicted from the present method: the entrainment factor  $\lambda$  and the exit pressure  $p_i$ . Both quantities should depend on the parameters  $JR$  and  $d/D$ , if not sensitively on  $HR$ . Thus the assumption of constant values for  $\lambda$  and  $p_i$  in the calculations should be abandoned as soon as such information becomes available. Such information should also be used to determine the peak values of the suckdown force.

Evidently, additional experimental and theoretical works are needed to solve the lift-loss problem. In the experimental area, it is recommended that

1) careful measurements be made for the surface pressures, including  $p_i$ , for various meaningful values of  $h/D$ ,  $JR$ ,  $HR$ , and  $d/D$ ;

2) measurements of the flow entrainment and a determination of the entrainment factor of  $\lambda$  be conducted;

3) accurate determination of the flow patterns (e.g., Figs. 1a and 1b and the trapped doughnut-vortex pattern) and measurements of the lift losses be conducted;

4) measurements be conducted for the single jet first and extended to multijet cases.

Up to the present time most of the experimental studies have been directed toward determining lift losses. Very few measurements of the surface pressure distribution or of the flowfield have been attempted. It is believed that such measurements are needed, not only for a better understanding of the aerodynamics of lift loss, but also for the development of reliable prediction methods not yet available.

Further development of the prediction methods can be facilitated by obtaining analytical solutions of the lift-loss problem. The present method can be improved by solving for higher-order terms in the pressure distributions. It appears that solution of three-dimensional, turbulent Navier-Stokes equations, using computational fluid dynamic technique will be most useful. Such solutions will provide data for  $\lambda$  and  $p_i$  needed in the present method as well as pressure distributions valid over the entire disk surface. Thus the present method of pressure matching can be verified and possibly extended to multijet cases with complex aircraft configurations.

### Acknowledgments

The author expresses his appreciation to the Naval Air Systems Command for sponsorship of the work, to Dr. B.G. Newman of McGill University for bringing Dr. P.S. Moller's work to his attention, and to Robert E. Palmer of NADC for his valuable help in the computing work.

### References

- <sup>1</sup>Margason, R.J., "Review of Propulsion Induced Effects on Aerodynamics of Jet V/STOL Aircraft," NASA TN D-5617, 1970.
- <sup>2</sup>Walters, M. and Henderson, C., "V/STOL Aerodynamics Technology Assessment," NADC-77272-60, May 1978.
- <sup>3</sup>Yen, K.T., "On the Vertical Momentum of the Fountain Produced by Vertical Multi-Jet Impingement," NADC-79273-60, Nov. 1979; see also, *Journal of Aircraft*, Vol. 18, Aug. 1981, pp. 650-654.
- <sup>4</sup>Yen, K.T., "Research on the Jet-Induced Lift Losses for V/STOL Aircraft in Hover," NADC-81238-60, Aug. 1981.
- <sup>5</sup>Kuhn, R.E., "An Empirical Method for Estimating Jet-Induced Lift Losses of V/STOL Aircraft Hovering In and Out-of-Ground Effect; Effects of Planform and Arrangements of Multiple Jets on Low Wing, Vertical Jet Configurations," Rept. R-AMAC-105, Dec. 1978.
- <sup>6</sup>Karema, A. and Ramsey, J.C., "Aerodynamic Methodology for the Prediction of Jet-Induced Lift in Hover," CASD-FRR-73-012, 1973.
- <sup>7</sup>Wyatt, L.A., "Static Tests of Ground Effect on Planforms Fitted with a Centrally-Located Round Lifting Jet," C.P. 749, ARC, British Ministry of Aviation, 1964.
- <sup>8</sup>Spreemann, K.P. and Sherman, I.R., "Effects of Ground Proximity on the Thrust of a Simple Downward-Directed Jet Beneath a Flat Surface," NACA TN 4407, 1958.
- <sup>9</sup>Gelb, G.H. and Martin, W.A., "An Experimental Investigation of the Flow Field about a Subsonic Jet Exhausting into a Quiescent and a Low Velocity Air Stream," *Canadian Aeronautics and Space Journal*, Vol. 15, Oct. 1966, pp. 333-342.
- <sup>10</sup>Milne-Thomson, L.M., *Theoretical Aerodynamics*, 2nd ed., Macmillan and Co., New York, 1949, pp. 513-515.
- <sup>11</sup>Moller, P.S., "Radial Flow Without Swirl Between Parallel Discs," *The Aeronautical Quarterly*, Vol. 14, May 1963, pp. 163-186.

*From the AIAA Progress in Astronautics and Aeronautics Series . . .*

## INJECTION AND MIXING IN TURBULENT FLOW—v. 68

*By Joseph A. Schetz, Virginia Polytechnic Institute and State University*

Turbulent flows involving injection and mixing occur in many engineering situations and in a variety of natural phenomena. Liquid or gaseous fuel injection in jet and rocket engines is of concern to the aerospace engineer; the mechanical engineer must estimate the mixing zone produced by the injection of condenser cooling water into a waterway; the chemical engineer is interested in process mixers and reactors; the civil engineer is involved with the dispersion of pollutants in the atmosphere; and oceanographers and meteorologists are concerned with mixing of fluid masses on a large scale. These are but a few examples of specific physical cases that are encompassed within the scope of this book. The volume is organized to provide a detailed coverage of both the available experimental data and the theoretical prediction methods in current use. The case of a single jet in a coaxial stream is used as a baseline case, and the effects of axial pressure gradient, self-propulsion, swirl, two-phase mixtures, three-dimensional geometry, transverse injection, buoyancy forces, and viscous-inviscid interaction are discussed as variations on the baseline case.

200 pp., 6×9, illus., \$17.00 Mem., \$27.00 List

TO ORDER WRITE: Publications Dept., AIAA, 1290 Avenue of the Americas, New York, N. Y. 10019